INTERNATIONAL JOURNAL OF PHARMACEUTICAL, CHEMICAL AND BIOLOGICAL SCIENCES

Available online at www.ijpcbs.com

Research Article

PHASE STRUCTURE, DIELECTRIC AND PIEZOELECTRIC PROPERTIES OF MODIFIED-PZT CERAMICS NEAR THE MORPHOTROPIC PHASE BOUNDARY

Necira Zelikha[1], Boutarfaia Ahmed[1, 2], Kharief Amel[3], Menasra Hayet[1], Bounab Karima[1], Abba Malika[1], Abdessalem Nora[1] and Meklid Abdelhek[1]

[1]Laboratoire de Chimie Appliquée LCA, Département des Sciences de la Matière, Université de Biskra Algérie.
[2]Université de Ouargla, Algérie.
[3]Laboratoire de Chimie Moléculaire, Université Mentouri Constantine, Algérie.

ABSTRACT

Modified-PZT ceramics with a formula $Pb[(Zr_xTi_{(0.98-x)}(Mg_{1/3}Nb_{2/3})_{0.01}(Ni_{1/3}Sb_{2/3})_{0.01}]O_3$(doped with hardeners : Mg^{2+}; Ni^{2+} and softeners : Nb^{5+}; Sb^{5+} ions) abbreviated as PZT-PMN-PNS quaternary system with varying Zr/Ti ratios in the range: $0.42 \leq x \leq 0.54$ located near the morphotropic phase boundary (MPB) were prepared by conventional solid state process. The phase structure, dielectric and piezoelectric properties of the system were investigated. Phase analysis using X-ray diffraction (XRD) indicated that the phase structure of sintered PZT-PMN-PNS ceramics was transformed from tetragonal to rhombohedral, with Zr/Ti ratio increased in system. The MPB, in which the tetragonal and rhombohedral phases coexist, is in a composition range of Zr content from 48 to 52 mol%. Scanning electron micrographs of sintered ceramic surfaces (at 1180°C) showed the dense and uniform microstructure for composition close to MPB (Zr/Ti = 50/48) with apparent density of 7.9 g/cm^3 (≈ 98 % of the theoretic density). For 1.0 mol% (Mg, Nb) and 1.0 mol% (Ni, Sb) doped PZT composition with x = 50, electrical properties were significantly improved. The main parameters of Pb $[Zr_{0.50}Ti_{0.48}(Mg_{1/3}Nb_{2/3})_{0.01}(Ni_{1/3}Sb_{2/3})_{0.01}]O_3$ piezoceramic system are: $\varepsilon_{r(max)}$ = 16624.79 at 1 kHz, Tc = 340 ◦C, tgδ = 0.86 %, ρ = 22.85 (*10^6 Ω.cm), $-d_{31}$ = 120.4 pC/N, Kp = 0.69, Q_m = 461.9. The properties of this type of ceramics make it a very promising piezoelectric material for device applications.

Keywords: Modified PZT, Zr/Ti ratio, Conventional solid state process, Rhombohedral.

1. INTRODUCTION

Piezoelectric ceramics have attracted considerable attention because of their possible uses in device applications such as sensors, actuators and transducers[1-7]. A wide range of these applications are based on lead zirconate titanate ($PbZr_xTi_{1-x}O_3$ or PZT) complex perovskite ceramics[8,9]. Especially, the solid solution composition located near the rhombohedral (antiferroelectric PbZrO3)–tetragonal (ferroelectric PbTiO3) morphotropic phase boundary (MPB, $x \approx 0.5$), depending in Zr/Ti ratio possesses eminent piezoelectric characteristics[10-15]. Each application area of PZT piezoceramics requires a particular combination of electrical properties: dielectric permittivity (ε), dielectric losses (tgδ), mechanical quality factor (Q_m), electromechanical coupling coefficient (Kp), and piezoelectric factor (d_{31} and

d_{33}). Classically, the electrical properties of PZT ceramics are modulated by the incorporation of small amounts of cations (doping) (typically 0.5–2 mol %). Modification of PZT with suitable substitutions of single or multiple cations at Pb^{2+} and Zr^{4+}/Ti^{4+} sites helps in enhancing its physical and electrical properties. There are two principal categories of dopants[16-18]:

• Donor dopants (softeners) which are higher valence substituents like Nb^{5+} or Sb^{5+} in the place of (Zr^{4+}/Ti^{4+}) or Gd^{3+} or Eu^{3+} in the place of Pb^{2+} and cause the following changes of the characteristics of PZT: higher dielectric constant and losses (at room temperature); higher charge coefficient d_{31}/d_{33}; much lower mechanical quality factor Q_m and easy to depolarize by mechanical stress. The excess of positive charge in soft PZT is compensated by lead vacancies.

• Acceptor dopants (hardeners) which are lower valence substituents like Mg^{2+} or Fe^{3+} (B-site) or Na^{+} (A-site) and cause the following changes of the characteristics of PZT: lower dielectric constant and losses (at room temperature); lower d_{33}; much higher mechanical Q_m; difficult to depolarize by mechanical stress. The lack of positive charge in hard PZT is compensated by oxygen vacancies.

The complex doping of two or more elements is expected to combine the properties of donor doped and/or acceptor doped PZT, which could exhibit better stability or improved piezoelectric and dielectric properties than those of the single element doped PZT[19-23].

In the present study, to combine and to improve the electrical properties of PZT ceramics, a complex doping with more metal elements including acceptor (hardener) :Mg^{2+}; Ni^{2+} and donor (softener): Nb^{+5}; Sb^{+5} replaces Zr^{4+} or Ti^{4+} on the B-Site has been adopted. Compositionally modified-PZT ceramics with variable Zr/Ti ratios were prepared by the conventional solid state reaction process in which all starting oxides are mixed directly to fabricate electronic ceramics. The effects of Zr/Ti ratio on the properties of sintered PZT-PMN-PNS quaternary system ceramics were investigated systematically.

2. EXPERIMENTAL PROCEDURE

Compositionally modified-PZT [doped with hardeners (Mg^{2+}, Ni^{2+}) and softeners (Nb^{5+}, Sb^{5+}) on the B-Site], with a nominal composition of $Pb[(Zr_xTi_{(0.98-x)}(Mg_{1/3}Nb_{2/3})_{0.01}(Ni_{1/3}Sb_{2/3})_{0.01}]O_3$ containing different Zr/Ti ratios ($0.42 \leq x \leq 0.54$) ceramics of near the MPB compositions were prepared by the conventional solid-state reaction of metal oxides. Polycrystalline samples were obtained using reagent-grade raw materials form of high purity: Pb_3O_4 (99.0%), ZrO_2 (99. 0%), TiO_2 (99.0%), MgO (99.6% purity), Nb_2O_5 (99.95% purity), NiO (99.6% purity) and Sb_2O_3 (>99.0% purity). These oxides were mixed in stoichiometric proportions. The mixture powders were milled for approx. 4 hours in an acetone medium. After drying and crushing, the obtained powders were calcined on alumina plates at 800°C for 2 hours with heating and cooling rates of 2 °C/mn[24]. The calcined powders were crushed for a second time and pressed into discs of 13 mm diameter and ~1 mm thickness at a pressure of 3500 $Kg.cm^{-2}$ using a uniaxial hydraulic press. These pellets were then sintered in a closed alumina crucible at in the range between 1100 °C and 1200 °C for 2 hours. To prevent PbO volatilization from the disks, a PbO atmosphere was maintained by placing $PbZrO_3$ powders in the crucible. The density measurements of the sintered pellets were determined by the Archimedes method. Crystal structure and phases identification of the sintered specimens crushed into powders were carried out by X-ray diffractometers (X Pert Graphics and Simens D500) at room temperature using CuKα radiation. The compositions of the PZT-PMN-PNS phases were identified by analysis of the peaks [$(0\ 0\ 2)_T$, $(2\ 0\ 0)_R$, $(2\ 0\ 0)_T$] in a range of Bragg angles 2θ range (42°-47°) and compared with the information from the JCPDS database. The tetragonal (T), rhombohedral (R) and tetragonal–rhombohedral phases were characterized and their lattice parameters were also calculated and refined using the least square method. The size, shape and distribution of the grains were analyzed by using Scanning electron microscope (JEOL, JSM 6400). For electrical measurements, high-purity silver paste was painted on both sides of the samples at 750 °C for 30 min as electrodes. The dielectric response was measured at the frequency of 1 kHz using an automatic LCR meter (800 S. GWI, LTD) at a temperature range from 25 °C to 450 °C with a heating rate of 1 °C/mn. Samples for the piezoelectric measurements were poled in silicone oil at 120°C by applying a DC electric field of 30-40 kV/cm for 45 min and then aged for 24 h prior to testing. Piezoelectric properties were measured via the resonance-antiresonance method by measuring the frequencies corresponding to the minimum and maximum impedance of the sample using an impedance analyzer.

3. RESULTS AND DISCUSSIONS

3.1. Phase structure

Figure 1 shows the dependences of the measured density of the PZT-PMN-PNS ceramics as a function of sintering temperature. The measured densities of the PZT-PMN-PNS samples increase significantly with increasing sintering temperature achieving a maximum value at 1180 °C and then decrease. From this figure, it was concluded that optimal sintering temperature for all samples was 1180 °C.

Figure 2 (a)-(c) shows the SEM micrographs of the fractured surface of the PZT-PMN-PNS specimen with Zr/Ti ratio of 50/48 sintered from 1100 to 1180 °C for 2 h. The SEM images reveal that the increase of sintering temperature resulted in significant changes in the microstructure of the specimen. The images also show that the grain size of the specimen varied considerably from 0.637 to 1.361 μm. Interestingly, the density results can be correlated to the microstructure because low–density of sintered ceramic at 1100 °C contain many closed pores (Fig.2(a)), whereas high-density of sintered ceramic at 1180 °C show high degrees of grain close packing (Fig.2 (c)).

To investigate the phase formation and the crystal structure, the ceramics with optimum sintering temperature were examined by XRD. Figure 3 shows the room temperature XRD patterns of PZT-PMN-PNS samples sintered at 1180 °C with different Zr/Ti ratios. It is observed that a pure perovskite phase is obtained. The tetragonal, rhombohedral and tetragonal–rhombohedral phases are identified by an analysis of the peaks [002(tetragonal), 200 (tetragonal), 200 (rhombohedral)] in the 2θ range of 42–47° correlated with JCPDS file number 33-0784 (T) and JCPDS file number 73-2022 (R). The splitting of the (002) and (200) peaks indicates that they are the ferroelectric tetragonal phase (F_T), while the single (200) peaks consistent with the ferroelectric rhombohedral phase (F_R). A transition from the tetragonal to the rhombohedral phase is observed as Zr/Ti ratio increases. Previously, a similar behavior was also observed with increasing Zr content in modified PZT based ceramics.

The multiple peak separation method was used to estimate the relative fraction of coexisting phases. The relative phase fraction (M_R) was then calculated using the following equations[25]:

$$M_R = \frac{I_{R(200)}}{I_{R(200)} + I_{T(002)} + I_{T(200)}} \quad (1)$$

$$M_T = \frac{I_{T(200)} + I_{T(002)}}{I_{R(200)} + I_{T(002)} + I_{T(200)}} \quad (2)$$

Where I_R(2 00) is the integral intensity of the (200) reflection of the rhombohedral phase and I_T(2 00) and I_T(0 02) are the integral intensities of the(200) and (002) reflections of the tetragonal phase, respectively. Analysis of the relative phase fractions in the PZT–PMN–PNS ceramics indicates that the tetragonal and rhombohedral phases coexist in the composition range of $0.49 < x < 0.51$ as shown in Fig. 4. It can be seen clearly that the MPB is over abroad composition range. The width of the MPB in PZT systems has been extensively investigated and found to be related to the heterogeneous distribution of Zr^{4+} and Ti^{4+} cations on the B-site of the perovskite lattice (ABO_3). In addition, the tetragonal and rhombohedral phases may co-exist in one grain, so that even a grain which consists mainly of one phase may contain nuclei of the other phase[26].

Table 1 shows the lattice parameter values of a and c axes for each PZT–PMN–PNS composition calculated from the XRD patterns. It can be seen that the lattice structure changes from the tetragonal to the rhombohedral phase as the ratio of Zr to Ti increases. In the tetragonal phase, the lattice parameter a_T increases linearly, while the c_T parameter decreases with increasing Zr/Ti ratio. The variation of these parameters is related to the distortion of the tetragonal structure defined by the c_T/a_T ratio (Tab. 1), which decreases with increasing Zr content, also confirming the occurrence of phase transition from tetragonal to rhombohedral symmetry. The rhombohedral lattice parameter a_R appears to oscillate between 4.0344 and 4.1196 Å. The influence of the Zr/Ti ratio on the lattice structure can be explained by the difference between the ionic rays of Zr and Ti (0.72 and 0.605 Å, respectively)[27].

3.2. Dielectric properties

Temperature dependences of the dielectric constant (ε_r) of sintered PZT-PMN-PNS specimens with different Zr/Ti ratios are shown in Fig. 5. It can be seen that all the compounds undergo diffuse ferro-paraelectric phase transition at their respective phase transition temperatures.

The $\varepsilon_{r\,(max)}$ increases from Zr/Ti: 42/56 and shows maximum value at Zr/Ti: 50/48 and then decreases from Zr: 52 to 54, clearly indicating the maximum dielectric constant at MPB composition of Zr:50. In addition, a clear transition in T_{max}

(defined as the Curie temperature (T_c) at which ε_r is maximum at 1 kHz) is observed. It is noticed that an increase in Zr content leads to a decrease in T_c, most likely due to crystal structure of the materials was changed from tetragonal to rhombohedral, as shown in XRD patterns in Fig. 3. Also, this is due to the decrease of amount of PT content that has the relative high Curie temperature of 495 °C[9]. It is important to note that the values of T_c at morphotropic phase region were found to be nearly constant (~340 °C) in our choosing system (Fig.5).

Figure 6 shows Zr/Ti ratio dependence of dielectric losses (tanδ) of sintered PZT-PMN-PNS samples (at room temperature, 1 kHz). The values of tanδ decrease with increasing Zr from 0.42 to 0.50 mol% and then increase when Zr content increases further. When Zr/Ti ratio is 50/48 for the sample included in the morphotropic phase boundary (MPB), value of tanδ show the lower values of 0.0086.This lower values of dielectric losses is attributed to the high density and uniform microstructure of the sample (50/48/2) as observed in SEM graphs (Fig 2.c).

3.3 Piezoelectric properties

Obviously, the piezoelectric properties of sintered PZT-PMN-PNS ceramics are affected by Zr/Ti ratio. Fig. 7(a)-(c) shows the planar coupling factor (k_p), piezoelectric coefficient (d_{31}) and mechanical quality factor (Q_m) as a function of the Zr/Ti ratio.

PZT-PMN-PNS exhibits desirable *kp* and d_{31} values around the MPB. From the trend of the piezoelectricity, the sample reaches the maximum values of kp = 0.689, - d_{31}=120 pC/N, which coincides with the maxima of the dielectric constant when Zr/Ti ratio is 50/48 as listed in Tab.2. This maximum of piezoelectric activity can be explained by the presence of several directions of spontaneous polarization relating to the existence of the tetragonal and rhombohedral phases. The variation of Q_m is in accordance with the result of *kp* and d_{31}. Although, Q_m reflects the mechanical loss resulting to internal friction caused by moving of the tetragonal and rhombohedral phases near the MPB, a maximum value of 461.9 is obtained at Zr/Ti ratio of 50/48, clearly indicating the maximum mechanical quality factor at MPB. This is presumably attributed to the effect of hard and soft doping in the chosen PZT-PMN-PNS system. Complex doping with Mg^{+2}, Ni^{+2} (hard) and Nb^{+5}, Sb^{+5} (soft) ions at the B-site produces materials with the advantages of both soft and hard materials. The improved piezoelectric properties, i.e., enhanced Q_m with remaining relatively higher *kp*, are obtained in the modified-PZT composition.

The introduction of hard and soft dopants well modified the properties of the PZT ceramics and hence, with property selected additives and compositions, enhanced electrical properties for modified- PZT for various applications could be achieved. A similar behavior has also been observed in other systems with similar MPBs[28-31].

4. CONCLUSIONS

The effects of Zr/Ti ratio on phase structure and electrical properties of $Pb[(Zr_xTi_{(0.98\ -x)}(Mg_{1/3}Nb_{2/3})_{0.01}(Ni_{1/3}\ Sb_{2/3})_{0.01}]\ O_3$ quaternary system (abbreviated as PZT-PMN-PNS) were discussed. The present results can be summarized as follows:

1. High dense perovskite structure and a uniform microstructure of PZT-PMN-PNS ceramics were found at a sintering temperature of 1180°C.
2. The phase structure of system was transformed from tetragonal to rhombohedral with an increase of Zr/Ti ratio. The MPB of the tetragonal and rhombohedral phases in the present system was a broad composition region of $46 < x < 54$.
3. PZT-PMN-PNS exhibited high electrical properties around the MPB which was suitable for high-power applications was acquired with Zr/Ti = 50/48 at sintering temperature of 1180°C. The improved dielelectric and piezoelectric properties, i.e., enhanced Qm with remaining higher ε_r and kp for chosen system were obtained by modifying PZT composition with hard (Mg^{+2} Ni^{+2}) and soft (Nb^{+5} Sb^{+5}) dopants at B-site. The optimum values of ε_r, *tan δ*, d_{31}, *Kp*, Q_m, , T_c were 1665, 314 pC/N, 57.8%, 2614, 0.4%, 279 ◦C, respectively.

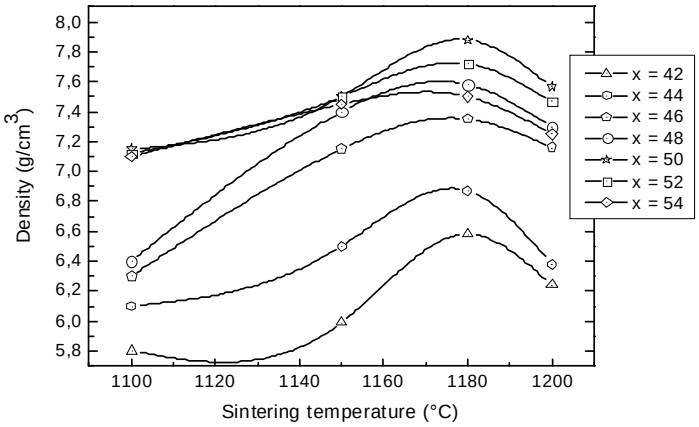

Fig. 1: Density of PZT-PMN-PNS ceramics with different Zr/Ti ratios as a function of sintering temperature

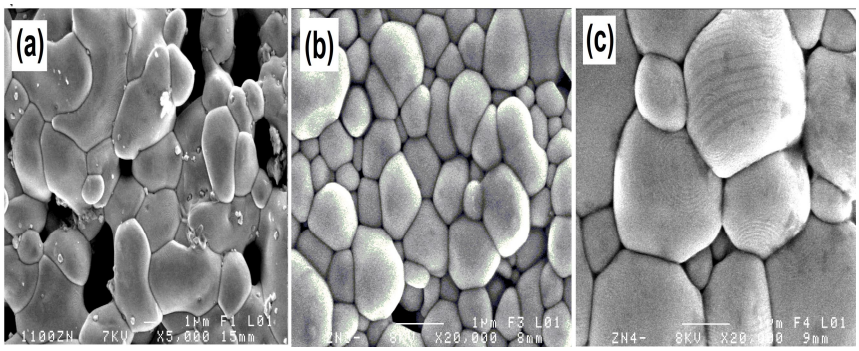

Fig. 2: SEM micrographs of $Pb[(Zr_{0.50}Ti_{0.48})(Mg_{1/3}Nb_{2/3})_{0.01}(Ni_{1/3}Sb_{2/3})_{0.01}]O_3$ specimen with increasing sintering temperature: (a) 1100°C, (b) 1150°C, and (c) 1180°C

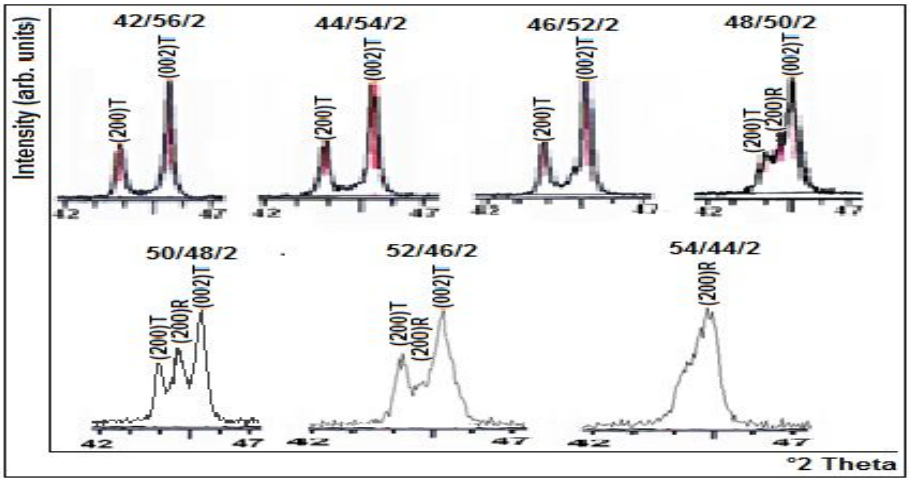

Fig. 3: XRD patterns of sintered PZT–PMN–PNS specimens with different Zr/Ti ratios (2θ range of 42–47°)

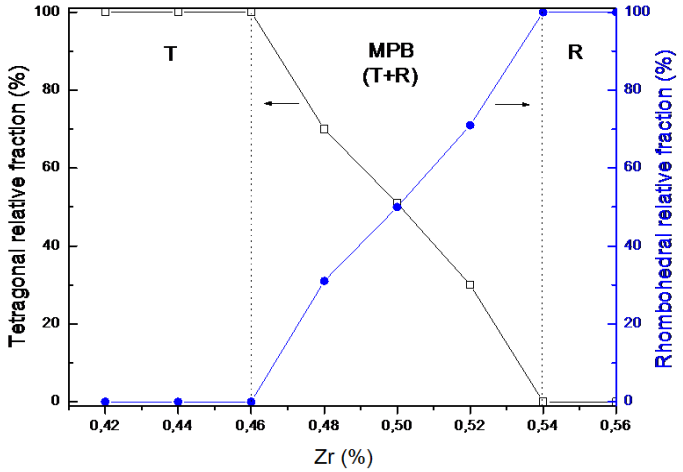

Fig. 4: Variation of the relative content of the tetragonal and rhombohedral phases with different Zr/Ti ratios in the PZT–PMN–PNS samples

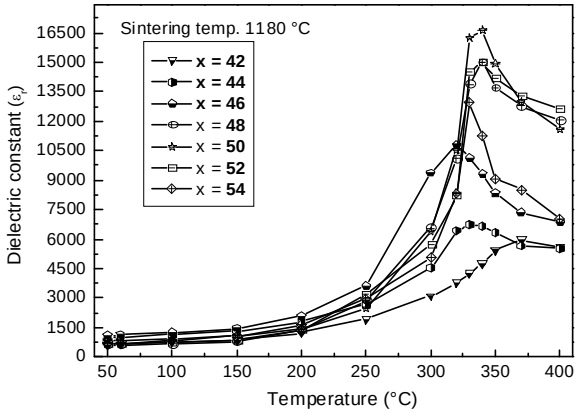

Fig. 5: Dielectric constant (ε_r) of sintered PZT-PMN-PNS specimens with different Zr/Ti ratio as a function of the temperature (f =1kHz)

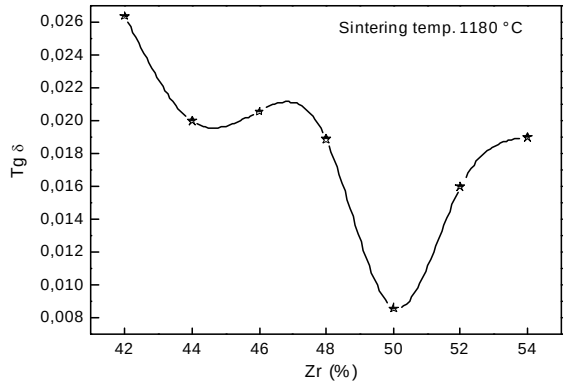

Fig. 6: Dielectric losses ($\tan\delta$) of sintered PZT-PMN-PNS specimens as a function of the Zr/Ti ratio (f=1 kHz)

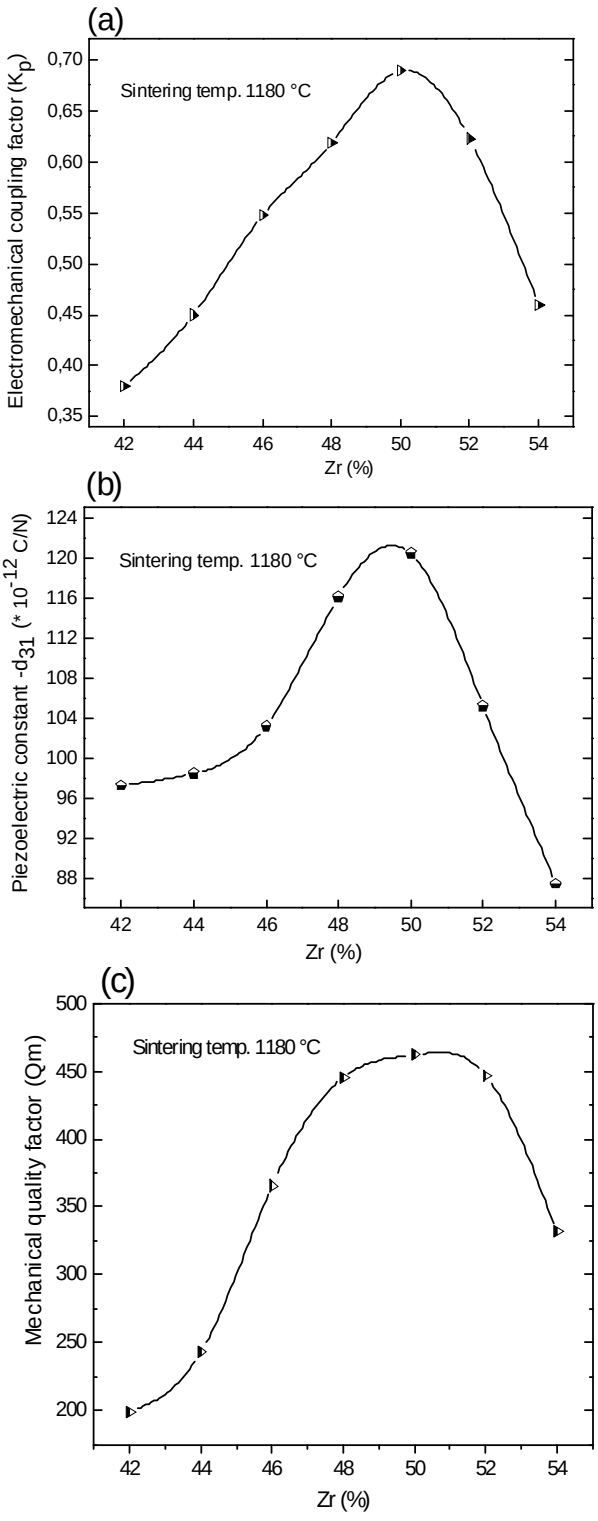

Fig. 7: d_{31}, kp and Qm of sintered PZT-PMN-PNS specimens as a function of the Zr/Ti ratio

Table 1: Comparison of crystal system (CS), lattice parameters, density (D) of PZT-PMN-PNS compound

Zr/Ti ratio	CS	Lattice parameters (Å)			c/a	D (g/cm³)
		$a_T = b_T$	c_T	a_R		
42/56	T	3.9844	4.1321	-	1.0370	6.58
44/54	T	3.9968	4.1258	-	1.0322	6.87
46/52	T	4.0128	4.1218	-	1.0271	7.35
48/50	T + R	4.0189	4.1199	4.0344	1.0251	7.58
50/48	T + R	4.0182	4.1183	4.0347	1.0249	7.89
52/46	T + R	4.0181	4.1182	4.1186	1.0249	7.72
54/44	R	-	-	4.1196	-	7.50

T-Tetragonal; R-Rhombohedral

Table 2: Dielectric and piezoelectric properties of sintered PZT–PMN–PNS ceramics near MPB at 1kHz

composition	ε_r at RT	$\varepsilon_{r(max)}$ at Tc	tg δ (%) at RT	ρ (*10⁶ Ω.cm)	Kp (pC/N)	d_{31} (pC/N)	Q_m
48/50/2	589.86	14978.90	1.89	18.440	0.618	116.08	445.5
50/48/2	818.30	16624.79	0.86	22.850	0.689	120.40	461.9
52/46/2	634.78	14999.9	1.60	14.595	0.623	105.15	446.8

ACKNOWLEDGEMENTS

Authors are thankful to Pr. A. Meghazzi, Director, Applied Chemistry Laboratory of University of Biskra (Algeria), for constant encouragement to this work. The authors also are greatly thankful to Pr. M. Poulain, Photonic materials Laboratory of University of Rennes1 (France), for providing some analyses help.

REFERENCES

1. M.E. Lines, A.M. Glass: Principles and applications of ferroelectrics and related materials (Oxford 1977).
2. Y. Xu, Ferroelectric materials and their applications, Elsevier Sci. Pub., Amsterdam, Netherlands, 1991).
3. G. H. Haertling, Ceramics materials for electronics: Processing, Properties and Application, New York, p.139 (1986).
4. G.H. Haertling, Ferroelectric ceramics: history and technology. J. Am. Ceram. Soc., 82, pp.797–818, (1999).
5. S. UEHA and Y. TOMIKAWA, Ultrasonic motors theory and applications (Oxford, New York, 1993).
6. Cross, L. E., Ferroelectric materials for electromechanical transducer applications. Jpn. J. Appl. Phys., 34, pp. 2525–2532, (1995).
7. A. G. Moulson and J. M. Herbert, Electroceramics, Second ed., John Wiley & Sons, Chichester, (2003).
8. B. Jaffe, R. S. Roth and S. Marzullo, Piezoelectric properties of lead zirconate–lead titanate solid solution ceramic ware. J. Res. Nat. Bur. Stand, 55(5), pp. 239–254, (1955).
9. B. Jaffe, W.R. Cook, H. Jaffe, Piezoelectric ceramics, Academic Press, New York, pp.135–171, (1971).
10. M. R. Soares, A. M. R. Senos and P. Q. Mantas, Phase coexistence region and dielectric properties of PZT ceramics. J. Eur. Ceram. Soc., 20, pp. 321–334, (2000).
11. N. Vittayakorn, G. Rujijanagul, X. L. Tan, M. A. Marquardt, and D. P. Cann, The morphotropic phase boundary and dielectric properties of the xPb(Zr1/2Ti1/2)O3-(1–x)Pb(Ni1/3Nb2/3)O3 perovskite solid solution. *J. Appl. Phys.* 96, p. 5103, (2004)
12. A. Babulescu, Eva. Barbulescu and D. Darb, Phase transition in PZT solid solutions. Ferroelectrics, 47, pp. 221–230, (1983).
13. A. Boutarfaia, Investigations of co-existence region in lead zirconate– titanate solid solutions: X-ray diffraction studies. Ceram. Int., 26, p. 583, (2000).
14. A. Boutarfaia and E. Bouaoud, Tetragonal and rhombohedral phase co-existence in the system: PbZrO3–PbTiO3–Pb(Fe1/5, Ni1/5,Sb3/5)O3. Ceram. Int., 22, pp. 281–286, (1995).
15. Noheda, B., Gonzalo, J. A., Cross, L. E., Guo, R., Park, S.-E., Cox, D. E. and Shirane, G., Tetragonal-to-monoclinic phase transition in a ferroelectric perovskite: The structure of $PbZr_{0.52}Ti_{0.48}O_3$. Physical Review B (Condensed Matter), 61, pp. 8687–8695, (2000).

16. B. Guiffard, E. Boucher, L. Lebrun, D. Guyomar, Characteristics of F doped PZT ceramics using different fluorine sources, Materials Science and Engineering B, 137, pp. 272–277, (2007).
17. Wei Hng, Q. and Hoon, H., Effects of dopants on the microstructure and properties of PZT ceramics, Mater. Chem. And Phys., 75, pp.151–156, (2002).
18. Qi Tan, Z Xu, Jie-Fanfg Li, and Dwight Viehland, Influence of lower-valent A-site modifications on the structure-property relations of Lead Zirconate Titanate. J. Appl. Phys., 80, (10), pp. 5866-74, (1996).
19. Byeong Woo Lee · Eon Jong Lee, Effects of complex doping on microstructural and electrical properties of PZT ceramics, J Electroceram, 17, pp. 597–602, (2006).
20. Garg, A. and Agrawal, D. C., Effect of rare earth (Er, Gd, Eu, Nd, and La) and bismuth additives on the mechanical and piezoelectric properties of lead zirconate titanate ceramics, Mater. Sci. and Eng. B, 86, pp.134–143, (2001).
21. S. Zahi, R. Bouaziz, N. Abdessalem, A. Boutarfaia, Dielectric and piezoelectric properties of PbZrO3-PbTiO3-Pb($Ni_{1/3}$ $Sb_{2/3}$)O_3 ferroelectric ceramics system, Ceram. Int. 29, pp.35-39, (2003).
22. Yeongho Jeong, Juhyun Yoo, Sangho Lee, Jaeil Hong, Piezoelectric characteristics of low temperature sintering $Pb(Mn_{1/3}Nb_{2/3})O_3$–$Pb(Ni_{1/3}Nb_{2/3})O_3$–$Pb(Zr_{0.50}Ti_{0.50})O_3$ according to the addition of CuO and Fe_2O_3, Sensors and Actuators A, (2006).
23. Pharatree Jaita, Anucha Watcharapasorn and Sukanda Jiansirisomboon, Effect of BNT addition on microstructure and mechanical properties of PZT ceramics, Journal of the Microscopy Society of Thailand, 24 (1), pp. 21-24 (2010).
24. Z. Necira, A. Boutarfaia, M. Abba and N. Abdessalem, Synthesis of PZT powder by conventional method at various conditions, European Physical Journal Conferences: Published by EDP Sciences, 29 00038 (2012).
25. G. H. Haerding and C. E. Land, Soc, 45, pp. 1-11, (1974).
26. A. Boutarfaia, S. Boudaren, A. Mousser and E. Bouaoud, Study of phase transition line of PZT ceramics by X-ray diffraction. Ceram. Int., 21, p. 391, (1995).
27. Chih-Yen Chen, Yi Hu, Hur-Lon Lin, Wan-Yi Wei, Influence of the sintering temperature on phase development in PMnN–PZT ceramics, Ceramics International, 33, pp.263–268, (2007).
28. Anurak Prasatkhetragarn, Muangjai Unruan, Athipong Ngamjarurojana, Yongyut Laosiritaworn, Supon Ananta, Rattikorn Yimnirun, David P. Cann, Effects of Zr/Ti ratio on dielectric and ferroelectric properties of $0.8Pb(Zr_xTi_{1-x})O_3$–$0.2Pb(Co_{1/3}Nb_{2/3})O_3$ ceramics, Current Applied Physics 9, pp. 802–806, (2009).
29. Haiyan Chen, Chunhua Fan, Phase structure and electrical properties of PSN–PMN–PZ–PT quaternary piezoelectric ceramics near the morphotropic phase boundary, Physica B , 405, pp.1941–1945, (2010).
30. Hongliang Du, Shaobo Qu , Jun Che, Zhibin Pei & Wancheng Zhou, Effect of Zr/Ti ratio on piezoelectric and dielectric properties of PNW–PMS–PZT ceramics, J Electroceram, 21, pp. 589–592, (2008).
31. N. Abdessalem, A. Boutarfaia, Effect of composition on the electromechanical properties of Pb [Zr_x $Ti_{(0.9\ -\ x)}$($Cr_{1/5}$, $Zn_{1/5}$, $Sb_{3/5})_{0.1}$]O_3 ceramics, Ceramics International, 33, 293–296, (2007).